Available online at www.sciencedirect.com

SciVerse ScienceDirect

Ceramics International 39 (2013) 1757–1764

CERAMICS INTERNATIONAL

www.elsevier.com/locate/ceramint

Structural, Mössbauer and electrical properties of nickel cadmium ferrites

M.M. Karanjkar[a], N.L. Tarwal[b,c,d], A.S. Vaigankar[e,*], P.S. Patil[b,*]

[a]Department of Physics, Vivekanand College, Kolhapur 416003, M.S., India
[b]Thin Film Materials Laboratory, Department of Physics, Shivaji University, Kolhapur 416004, M.S., India
[c]Research Institute for Solar and Sustainable Energies (RISE), Gwangju Institute of Science and Technology (GIST), Gwangju 500 712, Republic of Korea
[d]School of Information and Communications, Gwangju Institute of Science and Technology (GIST), Gwangju 500 712, Republic of Korea
[e]Department of Electronics, Shivaji University, Kolhapur 416004, M.S., India

Received 30 June 2012; received in revised form 6 August 2012; accepted 7 August 2012
Available online 23 August 2012

Abstract

A series of polycrystalline Ni–Cd ferrites were prepared by the ceramic method. The ferrite system exhibits cubic crystal structure. The lattice parameter dependence on Cd content obeys Vegard's law. Mössbauer spectroscopic studies of these ferrites were carried out by measuring average hyperfine field (H_n), quadruple splitting (Q_s) and isomer shift (I_s). These data are supported by the study of saturation magnetization, which suggests that Neel's two sublattice model governs the behavior of these ferrites up to about $x=0.2$ and after that triangular spin prevails. Moreover, the electrical properties were studied in the frequency range between 10 kHz and 15 MHz. For different compositions, the dielectric constant shows normal behavior with respect to frequency while loss tangent shows an anomalous behavior.

Keywords: C. Dielectric properties; D. Ferrite; Mössbauer spectroscopy; Hyperfine field

1. Introduction

Ferrites have replaced other magnetic alloys at high frequencies, due to coexistence of their magnetic properties and high resistivities. The ferrites have been proved to be industrially important materials. Ferrites constitute of double oxide of iron and another metal with a general formula MFe_2O_4, where M is divalent metal ion such as Mg^{2+}, Mn^{2+}, Co^{2+}, Ni^{2+}, Cd^{2+}, etc. The soft ferrites have been utilized in diverse technological applications such as microwave devices, high frequency cores, antennas, high frequency transformers, electronics, magnetic storage devices, ferrite wave absorber, multilayer chip inductor (MLCI), humidity sensors and thermo-junctions [1–4].

Enormous work has been done on polycrystalline Zn substituted ferrites [5–9] however, very little work is found in literature on Cd substituted soft ferrites. It is already pointed out that Cd substituted soft ferrites exhibit almost similar behavior as that of Zn substituted ferrites with some additional interesting properties such as electrical switching [10]. Moreover, due to high resistivity of $CdFe_2O_4$ the resistivity of the bulk will be considerably increased, which is one of the important aspects in developing soft ferrites. Also the properties of soft ferrites could be easily modified by the incorporation and suitable addition of divalent and trivalent cations in the spinel structure. Panicker et al. [11] and Wolska et al. [12] have synthesized the Ni–Cd ferrite system by the ceramic method and the co-precipitation method, respectively. The Mössbauer studies of Ni–Cd ferrites have been performed at a low temperature (5 K) by Greneche et al. [13]. Muthukumarasamy et al. have reported the concentration and temperature dependent Mössbauer studies of Ni–Cd ferrites [14]. Modi et al. [15] have reported the infrared (IR) studies and elastic properties of Ni–Cd ferrites synthesized by the co-precipitation technique.

*Corresponding authors. Tel.: +91 231 2609230; fax: +91 231 2691533.
E-mail addresses: tarwalnilesh@gmail.com (N.L. Tarwal), psp_phy@unishivaji.ac.in (P.S. Patil).

0272-8842/$ - see front matter © 2012 Elsevier Ltd and Techna Group S.r.l. All rights reserved.
http://dx.doi.org/10.1016/j.ceramint.2012.08.022

Also, the improvement in elastic properties of nickel ferrite by addition of Cd^{2+} has been reported. Ravinder et al. [16], and Ravinder and Manga [17] have studied the electrical properties such as conductivity and thermoelectric power studies as well as elastic properties of mixed Ni–Cd ferrites of various compositions.

Shelar et al. [18,19] have reported the chemical synthesis of Ni–Cd ferrites by the self-propagating auto combustion method and the structural, electrical and magnetic properties of fine grained Ni–Cd ferrites have been reported. Rangoliya et al. [20] have studied Cd substituted Ni ferrites with excellent magnetic properties. The structural and magnetic properties of nanosized Ni–Cd ferrite synthesized by the wet chemical co-precipitation method have been reported by Jadhav et al. [21]. Nikumbh et al. [22] have studied the structural, electrical and magnetic properties as well as cation distribution of cadmium-substituted nickel ferrite. Batoo et al. [23], Batoo [24] have investigated the influence of Al doping on the structural, electrical and Mössbauer properties of Ni–Cd-mixed ferrite. Kony [25] has investigated the dielectric properties of Al doped bulk Ni–Cd spinel ferrites. He reported that the distribution of Al at A and B sites has changed while changing the value of x, which has affected the dielectric properties of the ferrites. He also reported that two types of charge carriers are present at high temperature in the samples. Recently, rare earth metals (Gd and Sm) doping effects on the properties of nanocrystalline Ni–Cd mixed ferrite have been investigated by Jacob et al. [26] and Said et al. [27], respectively. Also, the structural, electrical and magnetic properties of these ferrites have been reported by them.

Several methods were employed to synthesize fine powder of ferrites such as the ceramic method [7,11,27], the co-precipitation method [12,15], the combustion method [18,19], the sol–gel method [23,26], ball milling [28], the standard double sintering ceramic technique [16,17,29], etc. Most of the co-precipitation methods are pH sensitive and sol–gel methods require alkoxide precursors and stringent process of gel product [22].

As pointed out above, very less work has been found in the literature on the $Cd_xNi_{1-x}Fe_2O_4$ system and further there are some discrepancies in the reported data. We have therefore planned to prepare the Ni–Cd ferrite samples by the ceramic method and to study their properties in detail. The preparation method influences final properties, especially the thermal treatment given to compounds in particular, and hence we expect changes in properties of $Cd_xNi_{1-x}Fe_2O_4$ ferrites.

Herein, we report structural, Mössbauer and electrical properties of the $Cd_xNi_{1-x}Fe_2O_4$ ferrite system synthesized via the ceramic method. The compositional dependences of lattice constant and Mössbauer spectra at room temperature have been studied and cation distribution in the $Cd_xNi_{1-x}Fe_2O_4$ ferrite has been reported. The AC electrical properties of the Ni–Cd ferrite system are also reported. The necessary parameters like dielectric constant (ε), resistivity (ρ) and loss tangent ($\tan\delta$) are determined at various frequencies ranging from 10 kHz to 15 MHz and obtained results are discussed here.

2. Experimental

Six specimen of the compositions $Cd_xNi_{1-x}Fe_2O_4$ with $x=0$, 0.2, 0.4, 0.6, 0.8 and 1.0 were prepared by the ceramic method. Powder forms of analytical reagent grade Fe_2O_3, CdO and NiO were mixed in appropriate proportions and presintered in air at 1023 K for 18 h. The resulting product is again powdered and fired at 1273 K for 48 h and slowly cooled to room temperature. This powder is then compressed in the form of pellets and further sintered at 1273 K for 20 h. The pellets were crushed to get the powder for X-ray and Mössbauer measurements.

The X-ray diffraction (XRD) patterns were obtained on a Phillips computerized diffractometer PW-1710 using CuK_α radiations, operated at 30 KV and 20 mA. Mössbauer spectra of these ferrites were recorded at room temperature using conventional constant acceleration drive coupled to an ND 100 multichannel analyzer operating in time mode. A 25 $mCI^{57}CO$:Rh source was used to record the spectra at room temperature. A metallic iron foil (25 μm) was used to calibrate the spectrometer and all isomer shifts were measured with respect to that of metallic iron. The AC electrical measurements were carried out in the frequency range 10 kHz to 15 MHz using a LCR meter bridge.

3. Results and discussion

3.1. XRD studies

Fig. 1 shows the XRD patterns recorded over 2θ values between 5° and 85° at room temperature for $Cd_xNi_{1-x}Fe_2O_4$ ferrite samples. The well-defined XRD

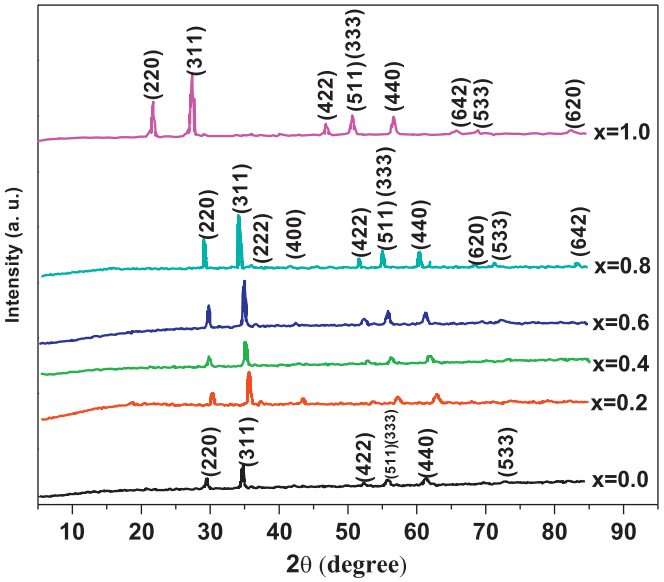

Fig. 1. X-ray diffractograms of the $Cd_xNi_{1-x}Fe_2O_4$ samples ($x=0.0$, 0.2, 0.4, 0.6, 0.8 and 1.0).

peaks with no ambiguous reflections can be immediately noted. From XRD it is confirmed that the synthesized ferrites exhibit polycrystalline nature with (220), (311), (222), (400), (422), (511), (333), (440), (620), (533) and (642) reflection planes. The observed reflections in the present case are in conformity with the spinel structure as well as to those of natural spinel crystal of $MgAl_2O_4$. The (111) plane completely disappeared in all samples. The reflections observed in XRD patterns of Ni–Cd ferrite samples for spinel structure confirm the preparation and formation of single phase, mixed $Cd_xNi_{1-x}Fe_2O_4$ ferrite.

Fig. 2 shows the variation of lattice parameter with Cd content and the values of lattice parameter (a) are provided in Table 1. From Fig. 2 it is seen that the lattice parameter dependence on the Cd^{2+} content exhibits linear variation. With increasing Cd content, the lattice constant goes on increasing. Thus, it obeys Vagard's law. In the earlier work of Panicker et al. [11] it was found to be deviated from Vagard's law; on the other hand Wolska's work showed that the compounds prepared by the co-precipitation method obey Vagard's law [12]. Since the ionic radii of Ni (0.074 nm) and Cd (0.097 nm) are such that with increasing Cd^{2+} content the lattice constant is expected to increase and further linear variation of lattice constant

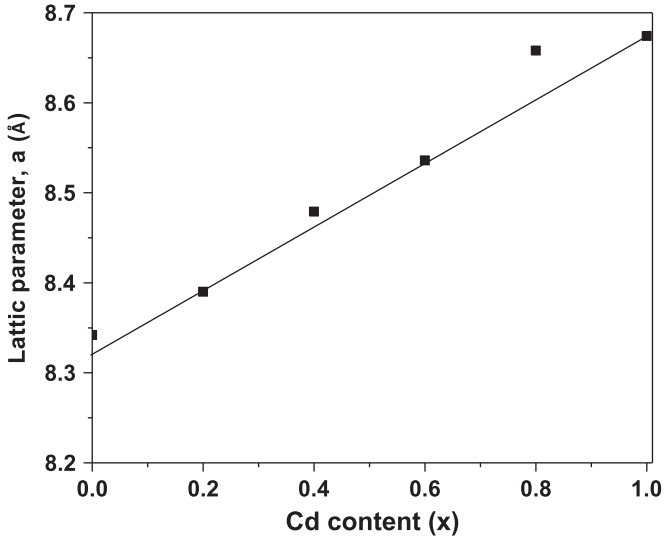

Fig. 2. Compositional dependence of lattice parameter (a) in $Cd_xNi_{1-x}Fe_2O_4$ (x=0.0, 0.2, 0.4, 0.6, 0.8 and 1.0) ferrite system.

Table 1
Lattice parameter a (Å) for the $Cd_xNi_{1-x}Fe_2O_4$ system with x=0.0, 0.2, 0.4, 0.6, 0.8 and 1.0.

x	Lattice parameter a (Å)
0.0	8.3707
0.2	8.4051
0.4	8.5011
0.6	8.5569
0.8	8.6362
1.0	8.6736

immediately suggests that the Cd^{2+} ions prefer to occupy the tetrahedral spinel positions, which is well known and that leads to suggest the cation distribution [30].

3.2. Mössbauer studies

Fig. 3. shows the Mössbauer spectra for the $Cd_xNi_{1-x}Fe_2O_4$ system obtained at room temperature (300 K). The Mössbauer data comprising I_s, Q_s and H_n are presented in Table 2. It can be noticed that, spectrum for composition x =1.0 (i.e. $CdFe_2O_4$) exhibits only one line with characteristic of Fe^{3+} ions on octahedral B-site showing paramagnetic behavior. Similar trend was observed in the case of x=0.8 composition. An alternate check to this was the measurement of transition temperature from ferri to paramagnetic regions, of two compositions and is found to be below room temperature. For composition x=0.6, a broad central line is clearly visible, which is superposed on Zeeman split sextets exhibiting relaxation behavior. This relaxation occurs at room temperature, which is much below the transition temperature (T_c=473 K). The spectral analysis suggests that this effect is due to domain wall oscillations. Similar explanations have been presented by Srivastava et al. [6], and Patil and Kulkarni [7] through simultaneous study of magnetization measurements and Mössbauer spectra of $Zn_xFe_{3-x}O_4$ and $Zn_xCu_{1-x}Fe_2O_4$ ferrites, respectively. These ferrites show relaxation effects for temperatures much lower than the Neel temperature (T_N). Since this effect occurs at $T < T_N$, it cannot be accounted for by critical point fluctuations. They showed that these effects arise due to magnetic relaxation processes associated with the domain-wall oscillation.

For remaining compositions x=0.4, 0.2 and 0.0, the spectra show normal Zeeman split sextets. To assign spectra to the Fe^{3+} in tetrahedral and octahedral interstices, an external magnetic field should be applied in a direction perpendicular to γ emission for complex spectra obtained in tetragonal and cubic $CuFe_2O_4$, respectively. When this happens, hyperfine field at the nuclei on octahedral sites decreases while hyperfine field at the nuclei on tetrahedral sites increases. This method has been utilized to identify and assign the complex spectra to the Fe^{3+} in the octahedral and tetrahedral sites [31]. It is not necessary to apply such method for present series of composition as spectra show clear cut sextets. Thus, for samples with x=0.4, 0.2 and 0.0 compositions, the splitting due to superposition of the hyperfine field spectra due to Fe^{3+} in octahedral and tetrahedral interstices is evident. Similar results are reported by Bhide [32] for the $NiFe_2O_4$ ferrite system. This is characteristic of Fe^{3+} ions on the tetrahedral A-sites and other due to Fe^{3+} ions on the octahedral B-sites. The intensities of these lines are equal suggesting that equal amounts of Fe^{3+} ions are distributed on both A and B sites; therefore, entire Ni is transferred to octahedral sites. The site preference of Cd^{2+} ions is well known to be for tetrahedral A-sites and therefore this leads to suggest the cation distribution in the $Cd_xNi_{1-x}Fe_2O_4$

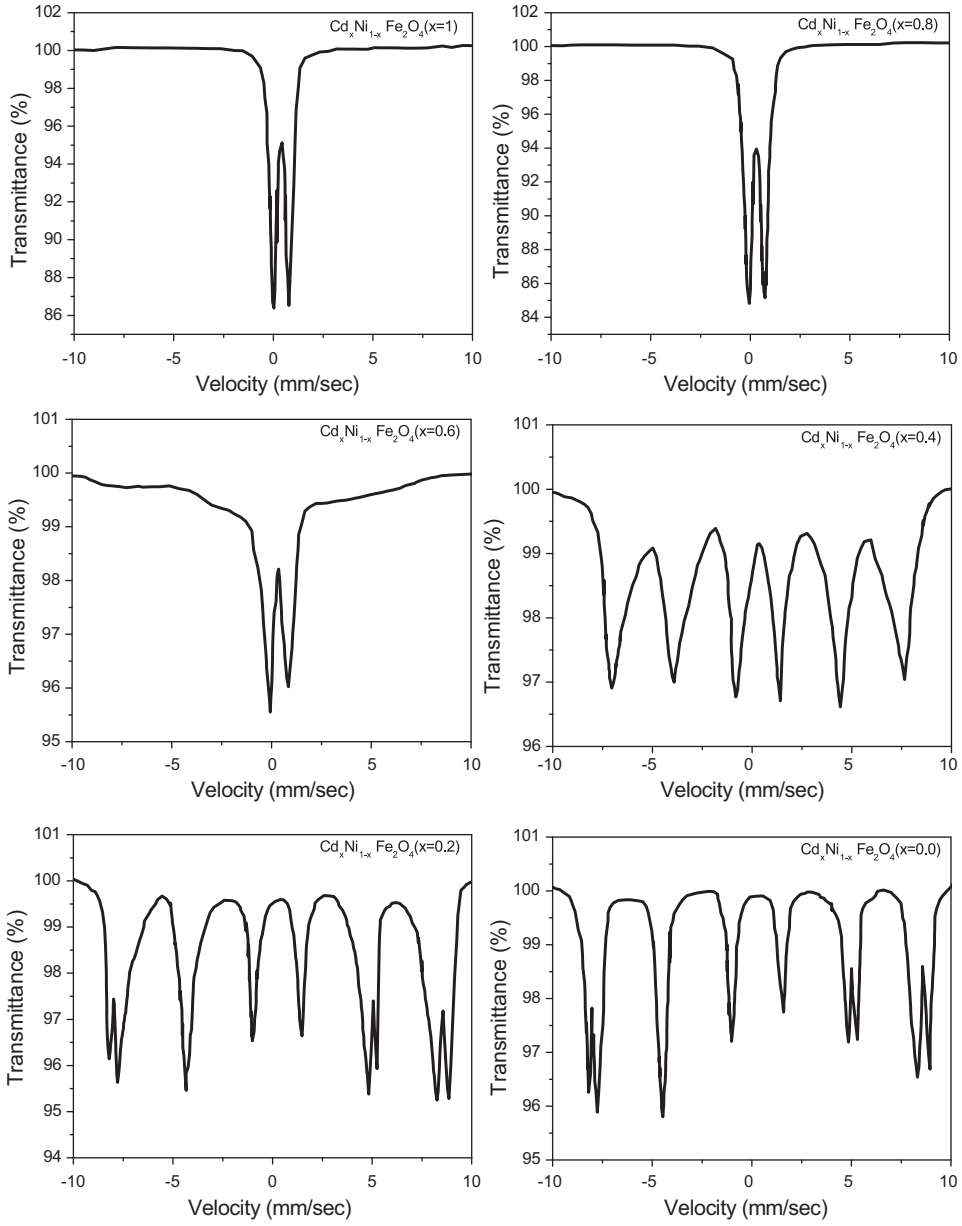

Fig. 3. Room temperature (300 K) Mössbauer spectra of $Cd_xNi_{1-x}Fe_2O_4$ ($x=0.0$, 0.2, 0.4, 0.6, 0.8 and 1.0) ferrite compositions.

Table 2
Mössbauer parameters, n_B and Y–K angles for $Cd_xNi_{1-x}Fe_2O_4$ at 300 K.

x	Average isomer shift δ_s (mm/s)	Average quadrupole splitting Q_s (mm/s)	Average hyperfine field H_n (kOe)	n_B 300 K (μB)	Y–K angles
0.0	0.2875	0.0125	514.02	2.11	0°
0.2	0.25	0.05	483.06	3.42	0°
0.4	0.22	0.025	449.00	2.93	220° 31’
0.6	Relaxation spectrum		–	2.07	520° 30’
0.8	0.35	0.80	–	–	–
1.0	0.38	0.70	–	–	–

system of the type,

$$(Cd_x^{2+}Fe_{1-x}^{3+})^{A}[Ni_{1-x}^{2+}Fe_{1+x}^{3+}]^{B}O_4^{2-} \quad (1)$$

The average hyperfine field data with Cd concentration is presented in same table and corresponding composition dependence is shown in Fig. 4. It can be seen that H_n decreases with increasing Cd concentration up to $x<0.4$. We have not separately shown H_n for A and B sites; however, the trend of variation of H_n with x is obvious and is similar to the observations made for other ferrite systems. This behavior can be attributed to possible change of spin orientation in Cd and Zn substituted ferrites. Therefore, in the present system the concentration dependence of average H_n can be attributed to canting of spins

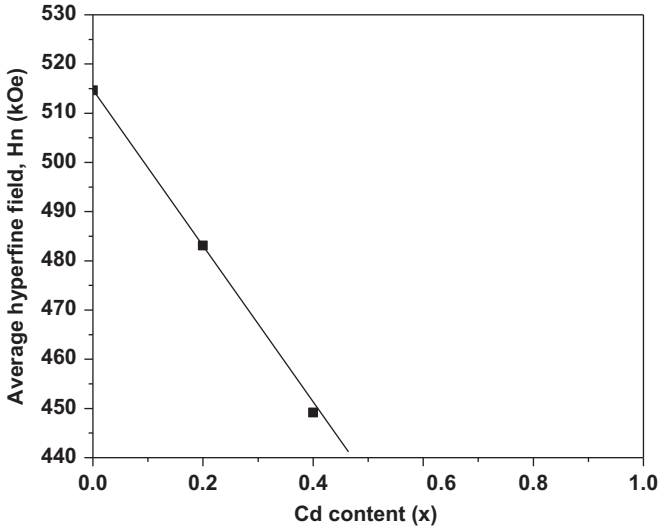

Fig. 4. Plot of average hyperfine field vs. cadmium content (x) at 300 K of $Cd_xNi_{1-x}Fe_2O_4$ (x=0.0, 0.2, 0.4, 0.6, 0.8 and 1.0) ferrite compositions.

which gives rise to Yafet–Kittel (Y–K) angles, suggesting A–B and B–B superexchange interactions to be comparable in strength.

Y–K angles are computed from the data obtained in the hysteretic experiment using high loop tracer for same compounds, using following equation:

$$n_B = (7+x)\cos \alpha yk - 5(1-x) \quad (2)$$

where x represents the Cd content. The saturation magnetic moment dependence on Cd concentration is depicted in Fig. 5, which supports the above argument that Bohr magneton (n_B) values initially increase with increasing Cd content, supporting Neel's two sublattice model, reaches to maximum and then decrease at about $x<0.2$ continuously, suggesting change of spin and prevalence of the canted spin arrangement effect in this compound after Cd content.

From Table 2, it can be seen that there is an increment in the Q_s value. Muthukumarasamy et al. [14] have also observed similar behavior for Ni–Cd systems prepared by the ceramic method. The reported values of oxygen parameter ('u') for $NiFe_2O_4$ and $CdFe_2O_4$ are 0.381 [33] and 0.391 [9], respectively. It suggests that the increment in Q_s values with Cd content may be due to increase in 'u' parameter of the compositions.

3.3. AC resistivity studies

To understand the conduction mechanism and the hopping of charge carriers responsible for the conduction mechanism, the variation of AC resistivity (ρ) as a function of frequency was calculated. The conduction mechanism of ferrites is considered as hopping motion of the electron between Fe^{2+} and Fe^{3+} over the octahedral site of spinel lattice [18,34,35]. When jumping frequency is of appropriate magnitude, a loss peak is observed. Presence of

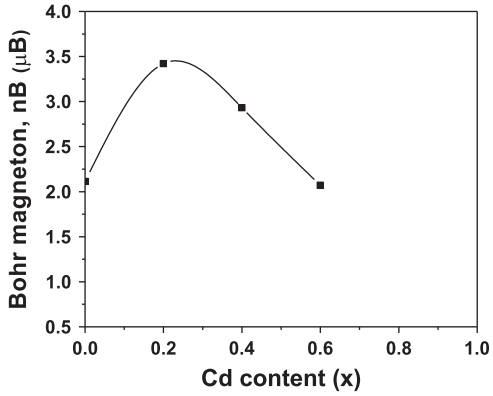

Fig. 5. Variation of Bohr magneton (n_B) with different Cd contents.

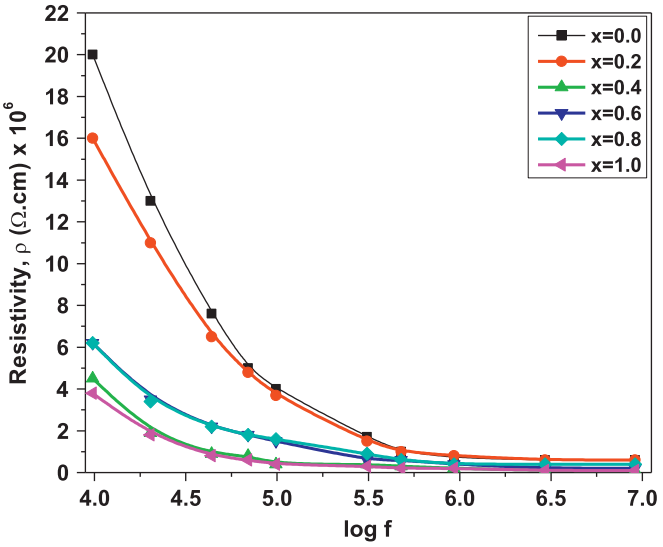

Fig. 6. Variation of AC resistivity with frequency of $Cd_xNi_{1-x}Fe_2O_4$ (x=0.0, 0.2, 0.4, 0.6, 0.8 and 1.0) ferrite compositions.

oxygen rich layers causes heterogeneity of the ferrites, which further contribute to an electrical conductivity. The electrical conductivity decreases from interior to the surface and would give rise to asymmetric distribution of relaxation times. For our sample, except x=0.0 i.e., $NiFe_2O_4$, there is possibility of some heterogeneity during the sintering process. This may arise from compositional variation and defect formation in samples. Compositional variation may change the amount of Fe^{2+} and Fe^{3+} in the samples. In this way, the position and magnitude of a loss peak observed in our sample may be influenced by compositional variation, inclusive impurities and jumping frequency among the divalent ion pairs on B-sites of the spinel lattice. Patil et al. [36] have observed similar peak for their dielectric studies for Li.

From Fig. 6, it is seen that the ρ decreases as frequency increases and remains constant at a higher value of frequency for all the samples. Explanation for the dispersion in ρ with frequency is provided by Koops [37]. He attributed the ferrite compact as a multilayer capacitor in which ferrite grains and grain boundaries have different

properties. The reactance of that multilayer capacitor is affected by applied AC field. When reactance is less affected by applied AC field then conductivity would appear practically independent of frequency at lower values. After certain frequency, this effect of the multilayer capacitor is changed linearly, and therefore AC resistivity would exhibit dispersion. The multilayer region of ferrite may contain a mixture of multi-domain (MD) and single-domain (SD) grains. This mixture gives rise to inhomogeneity within the material [35]. Thus, the presence of MD and SD grains may have some effect on AC resistivity. The dispersion characteristics of ρ for this series are in general agreement with the Koops model showing relaxation due to interfacial polarization.

Fig. 7 shows the frequency dependence of dielectric constant (ε). From Fig. 7, it is seen that the ε decreases with increase of frequency which is rather a normal behavior. The dispersion for sample $x=0$ is minimum and addition of Cd^{2+} tends to increase dispersion of the dielectric constant. According to Koops [37] dielectric is an inhomogeneous medium of Maxwell–Wagner [two layers] type. He has imagined the conducting and insulating region inside the sample. These regions are capacitors and resistors, which form an equivalent parallel resistor–capacitor circuit. The interrelationship between dielectric and conducting properties of the regions changes with frequency and effectively may constitute the dispersion by polarization. Normal dielectric behavior of the ferrites can be explained on the basis of mechanism of the polarization process in ferrites. According to Rabkin and Novikova [38], the polarization process in the ferrites takes place through a mechanism similar to the conduction process. The decrease in polarization i.e., decrease of dielectric constant with frequency takes place when jumping frequency of electric charge carriers cannot follow the alternation of electric field beyond critical value [39].

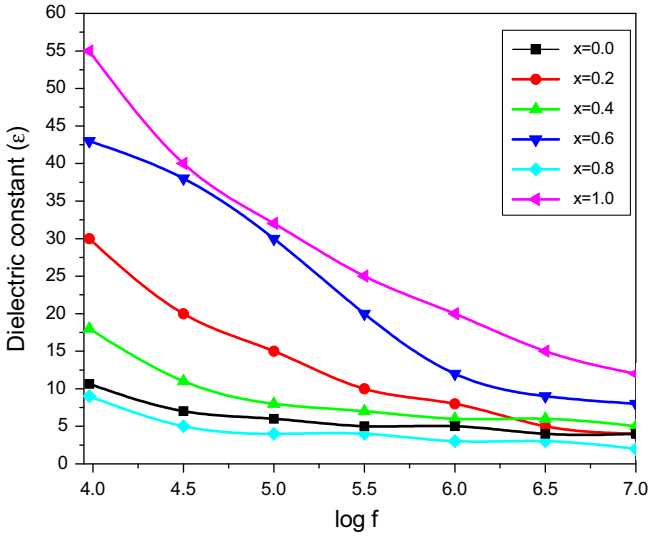

Fig. 7. Variation of dielectric constant (ε) with frequency of $Cd_xNi_{1-x}Fe_2O_4$ ($x=0.0$, 0.2, 0.4, 0.6, 0.8 and 1.0) ferrite compositions.

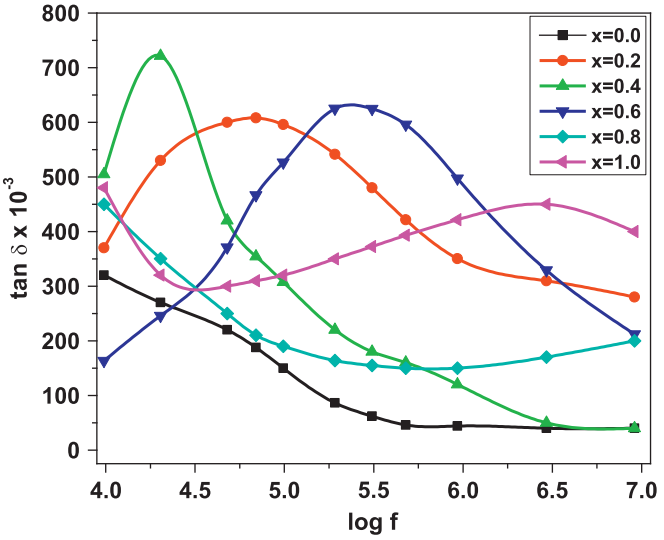

Fig. 8. Variation of loss tangent ($\tan\delta$) with frequency of $Cd_xNi_{1-x}Fe_2O_4$ ($x=0.0$, 0.2, 0.4, 0.6, 0.8 and 1.0) ferrite compositions.

For present series of samples, change in dielectric constant is more at low frequencies for all samples and remains constant after the frequency of 10 MHz.

The large value of ε at lower frequency is due to predominance of species like Fe^{2+} ions, interfacial dislocation pile ups, oxygen vacancies, grain boundary defects, etc. The decrease in ε with frequency is natural. This is due to the fact that any species contributing to polarizability is found to lag behind the applied field at higher and higher frequencies. Similar dielectric behavior was also observed by Kharabe et al. [29] for Li–Ni–Cd ferrites and Ravinder [40] for Li–Cd ferrites.

The variation of loss tangent ($\tan\delta$) with frequency is shown in Fig. 8. The graph shows a peak for compositions from $x=1.0$ to 0.2, while for composition $x=0.0$ i.e., $NiFe_2O_4$ does not show such type of peak. The loss tangent peaks are observed at lower frequency side from the compositions $x=0.2$–0.6. The loss factor initially increases with frequency up to 0.608, 0.722 and 0.632, correspondingly for these compositions and then decreases. The samples with compositions $x=0.8$ and 1.0 show some different behaviors. The loss tangent initially decreases to 0.147 and 0.290, correspondingly for these compositions as frequency increases and becomes maximum for the frequency near about 10 MHz, again decreases as further frequency increases. On the contrary, Shelar et al. [18] have reported the decrement in loss tangent factor with increase in frequency.

4. Conclusions

$Cd_xNi_{1-x}Fe_2O_4$ ferrites have been prepared by using the ceramic method with different concentrations of Cd ($x=0$, 0.2, 0.4, 0.6, 0.8 and 1.0). From XRD analyses, it is confirmed that all ferrites are polycrystalline having cubic crystal structure. The lattice parameter dependence on Cd

content obeys Vegard's law. The data from Mössbauer spectroscopic study of the ferrites was further supported by study of saturation magnetization in samples, which suggested Neel's two sublattice models govern the behavior of these ferrites up to about $x=0.2$ and after that triangular spin prevails. The dielectric constant is found to decrease with increase in frequency. The small polaron type of conduction was confirmed from AC resistivity measurements. The loss tangent variation with frequency reflects an anomalous behavior for different compositions.

Acknowledgment

The authors wish to acknowledge the UGC, New Delhi for the financial support through the UGC–DSA 1st phase programme (2010–2015), DST through the FIST programme (2002–2007) and the UGC–ASIST programme (2005–2010). One of the authors (N.L.T.) is thankful to the University Grants Commission, New Delhi for the 'Research Fellowship in Science for Meritorious Students to Promote Quality Research in Universities' under the UGC–DRS (SAP)–II programme.

References

[1] R. Alcantra, M. Jaraba, P. Lavela, J.L. Tirado, J.C. Jumas, J. Olivier-Fourcade, Changes in oxidation state and magnetic order of iron atoms during the electrochemical reaction of lithium with $NiFe_2O_4$, Electrochemistry Communications 5 (2003) 16–21.

[2] L. Satyanarayana, K.M. Reddy, S.V. Manorama, Nanosized spinel $NiFe_2O_4$: a novel material for the detection of liquefied petroleum gas in air, Materials Chemistry and Physics 82 (2003) 21–26.

[3] B.S. Randhawa, H.S. Dosanjh, Manpreet Kaur, Preparation of spinel ferrites from citrate precursor route—A comparative study, Ceramics International 35 (2009) 1045–1049.

[4] A.M. Ghozza, H.G. El-Shobaky, Effect of Li_2O-doping of CdO/Fe_2O_3 system on the formation of nanocrystalline $CdFe_2O_4$, Materials Science and Engineering: B 127 (2006) 233–238.

[5] S. Thakur, S.C. Katyal, M. Singh, Improvement in electric and dielectric properties of nanoferrite synthesized via reverse micelle technique, Applied Physics Letters 91 (2007) 262501–262503.

[6] C.M. Srivastava, S.N. Shringi, R.G. Srivastava, Mössbauer study of relaxation phenomena in zinc–ferrous ferrites, Physical Review B 14 (1976) 2041–2050.

[7] V.U. Patil, R.G. Kulkarni, Magnetic properties of Cu–Zn ferrite investigated by Mössbauer spectroscopy, Solid State Communications 31 (1979) 551–555.

[8] A.A. Mostafa, G.A. El-Shobaky, E. Girgis, Effects of ZnO-doping on structural and magnetic properties of $CdFe_2O_4$, Journal of Physics D: Applied Physics 39 (2006) 2007–2014.

[9] M. Chakrabarti, D. Sanyal, A. Chakrabarti, Preparation of $Zn_{(1-x)}Cd_xFe_2O_4$ ($x=0.0$, 0.1, 0.3, 0.5, 0.7 and 1.0) ferrite samples and their characterization by Mössbauer and positron annihilation techniques, Journal of Physics: Condensed Matter 19 (2007) 236210–236220.

[10] U.V. Chhaya, B.V. Mistry, K.H. Bhavsar, M.R. Gadhvi, V.K. Lakhani, K.B. Modi, U.S. Joshi, Structural parameters and resistive switching phenomenon study on $Cd_{0.25}Co_{0.75}Fe_2O_4$ ferrite thin film, Indian Journal of Pure and Applied Physics 49 (2011) 833–840.

[11] V.G. Panicker, R.V. Upadhyay, S.N. Rao, R.G. Kulkarni, Non-colinear spin structure in Ni–Cd ferrite system, Journal of Materials Science Letters 3 (1984) 385–387.

[12] E. Wolska, E. Riedel, W. Wolski, The evidence of $Cd_{2+x}Fe^{3+}_{1-x}[Ni^{2+}_{1-x}Fe^{3+}_{1-x}]O_4$ cation distribution based on X-ray and Mössbauer data, Physica Status Solidi(A) 132 (1992) K51–K56.

[13] J.M. Greneche, J. Teillet, H. Pascard, A mixed nickel–cadmium ferrite investigated by Mössbauer spectrometry, Journal of Magnetism and Magnetic Materials 140–144 (1995) 2087–2088.

[14] P. Muthukumarasamy, T. Nagarajan, A. Narayanasamy, Mössbauer study of the Ni–Cd ferrite system, Physica Status Solidi(A) 64 (1981) 747–754.

[15] K.B. Modi, M.K. Rangolia, M.C. Chhantbar, H.H. Joshi, Study of infrared spectroscopy and elastic properties of fine and coarse grained nickel–cadmium ferrites, Journal of Materials Science 41 (2006) 7308–7318.

[16] D. Ravinder, S.S. Rao, P. Shalini, Room temperature electric properties of cadmium-substituted nickel ferrites, Materials Letters 57 (2003) 4040–4042.

[17] D. Ravinder, T.A. Manga, Elastic behaviour of Ni–Cd ferrites, Materials Letters 41 (1999) 254–260.

[18] M.B. Shelar, P.A. Jadhav, S.S. Chougule, M.M. Mallapur, B.K. Chougule, Structural and electrical properties of nickel cadmium ferrites prepared through self-propagating auto combustion method, Journal of Alloys and Compounds 476 (2009) 760–764.

[19] M.B. Shelar, P.A. Jadhav, D.R. Patil, B.K. Chougule, Vijaya Puri, Chemical synthesis and studies on structural and magnetic properties of fine grained nickel cadmium ferrites, Journal of Magnetism and Magnetic Materials 322 (2010) 3355–3358.

[20] M.K. Rangoliya, M.C. Chhantbar, A.R. Tanna, K.B. Modi, G.J. Baldha, H.H. Joshi, Magnetic behaviour of nano-sized and coarse powders of Cd–Ni ferrites synthesized by wet-chemical route, Indian Journal of Pure and Applied Physics 46 (2008) 60–64.

[21] S.P. Jadhav, B.G. Toksha, K.M. Jadhav, N.D. Shinde, Effect of cadmium substitution on structural and magnetic properties of nano sized nickel ferrite, Chinese Journal of Chemical Physics 23 (2010) 459–464.

[22] A.K. Nikumbh, A.V. Nagawade, G.S. Gugale, M.G. Chaskar, P.P. Bakare, The formation, structural, electrical, magnetic and Mössbauer properties of ferrispinels, $Cd_{1-x}Ni_xFe_2O_4$, Journal of Materials Science 37 (2002) 637–647.

[23] K.M. Batoo, S. Kumar, C.G. Lee, Alimuddin, Finite size effect and influence of temperature on electrical properties of nanocrystalline Ni–Cd ferrites, Current Applied Physics 9 (2009) 1072–1078.

[24] K.M. Batoo, Microstructural and Mössbauer properties of low temperature synthesized Ni–Cd–Al ferrite nanoparticles, Nanoscale Research Letters 6 (2011) 499–505.

[25] D.E. Kony, Dielectric relaxation in Al-substituted Ni–Cd spinel ferrites, Egyptian Journal of Solids 27 (2004) 285–297.

[26] B.P Jacob, S. Thankachan, S. Xavier, E.M. Mohammed, Effect of Gd^{3+} doping on the structural and magnetic properties of nanocrystalline Ni–Cd mixed ferrite, Physica Scripta 84 (2011) 045702–045707.

[27] M.Z. Said, D.M. Hemeda, S.A. Kader, G.Z. Farag, Structural, electrical and infrared studies of $Ni_{0.7}Cd_{0.3}Sm_xFe_{2-x}O_4$ ferrite, Turkish Journal of Physics 31 (2007) 41–50.

[28] C.N. Chinnasamy, A. Narayanasamy, N. Ponpandian, R.J. Joseyphus, K. Chattopadhyay, K. Shinoda, B. Jeyadevan, K. Tohji, K. Nakatsuka, J.-M. Greneche, Ferrimagnetic ordering in nanostructured $CdFe_2O_4$ spinel, Journal of Applied Physics 90 (2001) 527–529.

[29] R.G. Kharabe, R.S. Devan, C.M. Kanamadi, B.K. Chougule, Dielectric properties of mixed Li–Ni–Cd ferrites, Smart Materials and Structures 15 (2006) N36–N39.

[30] I.H. Gul, W. Ahmed, A. Maqsood, Electrical and magnetic characterization of nanocrystalline Ni–Zn ferrite synthesis by co-precipitation route, Journal of Magnetism and Magnetic Materials 320 (2008) 270–275.

[31] B.J. Evans, S.S. Hafner, Mössbauer resonance of Fe^{57} in oxidic spinels containing Cu and Fe, Journal of Physics and Chemistry of Solids 29 (1968) 1573–1588.

[32] V.G. Bhide, Mössbouer Effect and its Application, Tata McGraw-Hill Publications, India, 1973, p. 236.

[33] K.G. Stanley, Oxide Magnetic Materials, Clarendon Press, Oxford, 1962.
[34] P.B. Belavi, G.N. Chavan, L.R. Naik, R. Somashekar, R.K. Kotnala, Structural, electrical and magnetic properties of cadmium substituted nickel–copper ferrites, Materials Chemistry and Physics 132 (2012) 138–144.
[35] S.R. Sawant, R.N. Patil, Dispersion of dielectric constant and resistivity of Cu_xZn_{1-x} Fe_2O_4 samples, Bulletin of Materials Science 4 (1982) 11–15.
[36] R.S. Patil, S.V. Kakatkar, S.A. Patil, P.K. Maskar, S.R. Sawant, Dielectric behaviour of $Li_{0.5}Zn_xTi_xFe_{2.5-2x}O_4$ ferrites, Physica Status Solidi (A) 126 (1991) K185–K189.
[37] C.G. Koops, On the dispersion of resistivity and dielectric constant of some semiconductors at audio frequencies, Physical Reviews 83 (1951) 121–124.
[38] L.I. Rabkin, Z.I. Novikova, Ferrites, Izvesttya Akademii Nauk Belorusskoi SSR, Minsk (1960) 146.
[39] A.D. Sheikh, V.L. Mathe, Anomalous electrical properties of nanocrystalline Ni–Zn ferrite, Journal of Materials Science 43 (2008) 2018–2025.
[40] D. Ravinder, Dielectric behaviour of lithium–cadmium ferrites, Physica Status Solidi (A) 129 (1992) 549–554.